

Seasonal footprints on ecological time series and jumps in dynamic states of protein configurations from a non-linear forecasting method characterization

Leonardo Reyes^{*1}, Kilver Campos², Douglas Avendaño², Lenin González-Paz³, Alejandro Vivas³, Ysaías J. Alvarado⁴, and Saúl Flores⁵

¹Laboratorio de Dinámica no-lineal y Sistemas Complejos, Centro de Física, Instituto Venezolano de Investigaciones Científicas (IVIC), República Bolivariana de Venezuela.

²Laboratorio de Física de Fluidos y Plasmas, Centro de Física, Instituto Venezolano de Investigaciones Científicas (IVIC), República Bolivariana de Venezuela.

³Laboratorio de Biocomputación. Centro de Biomedicina Molecular. Instituto Venezolano de Investigaciones Científicas (IVIC). Maracaibo, Edo Zulia, República Bolivariana de Venezuela.

⁴Laboratorio de Química Biofísica Teórica y Experimental. Centro de Biomedicina Molecular. Instituto Venezolano de Investigaciones Científicas (IVIC). Maracaibo, Edo Zulia, República Bolivariana de Venezuela.

⁵Laboratorio Ecología de Suelos, Centro de Ecología, Instituto Venezolano de Investigaciones Científicas (IVIC), República Bolivariana de Venezuela.

June 21, 2024

Abstract

We have analyzed phenology data and jumps in protein configurations with the non-linear forecasting method proposed by May and Sugihara [1]. Full plots of prediction quality as a function of dimensionality and forecasting time give fast and valuable information about Complex Systems dynamics.

The notion of *prediction* is at the heart of the scientific method and of some theories about the mind (the predictive brain) [2]. In this article we explore decades of ecological data [3] and data from a model for sampling protein configurations using a dynamic indicator $\rho(E, T_p)$ introduced some time ago by May and Sugihara to distinguishing chaos from noise in time series [1] : ρ^2 is a number in the unit interval which quantify the quality of the predictions made by the non-linear forecasting method introduced by the authors. We have obtained valuable insights about such data when considering full plots of the quantity $\rho^2(E, T_p)$. Here E is a dimensionality parameter: in the forecasting method is the number of components

of vectors constructed with the data. We are trying to make a prediction T_p time steps into the *future* and the evaluation of that prediction is made with the quantity ρ . Characterizing the dynamics of a system is a basic goal in today's big data dominated scientific practice. In this work we have applied the method proposed by May and Sugihara to analyze data spanning decades of population dynamics of several species from a Venezuelan forest [3] and to analyze some aspects of protein dynamics [9].

Given some data series x_n the nonlinear forecasting model considers vectors of E components of the form $(x_i, x_{i-1}, x_{i-2}, \dots, x_{i-(E-1)})$ and constructs a prediction for the next x_{i+T_p} value in the series; the prediction's quality is quantified with the correlation ρ between observed and predicted values. Thus, for given data x_n , the quantity $\rho(E, T_p)$ is the basic output of the method [1].

In figure 1 we show $\rho^2(T_p)$ for *Hieronyma moritziana Pax & K. Hoffm* species for three values of the dimensionality parameter E , $E = 3$, $E = 7$ and $E = 12$, for signals of flowers and fruits populations as a function of time [3]. It can be appreciated that the seasonal time scale (one year) manifests itself at $E = 3$, where we obtain a periodic pattern. For $E = 12$ there is a decay in prediction quality as T_p increases, which is a signature of chaotic dynamics [1].

*corresponding author: leonardoivanrc@gmail.com

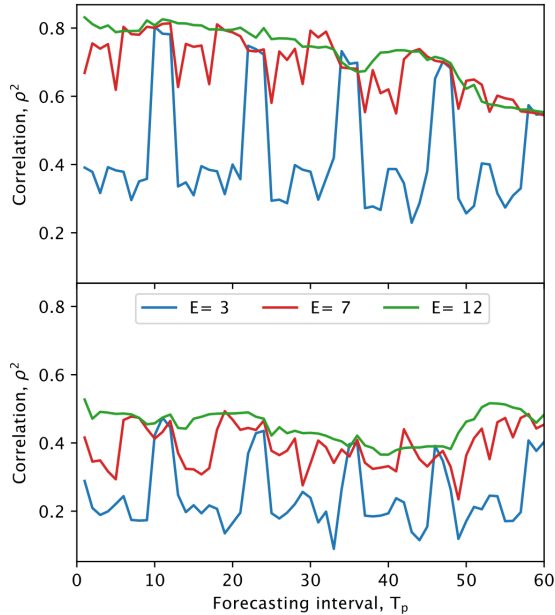


Figure 1: $\rho^2(T_p)$ for $E = 3$, $E = 7$ and $E = 12$ (see text). For $E = 3$ we get seasonal scales from the signal. For $E = 12$ we get chaotic dynamics from the signal for the case of flowers (top), and an *el niño* coupling for fruits (bottom). T_p is given in months. $E = 7$ is the first case outside the *small dimensionality* region in parameter space.

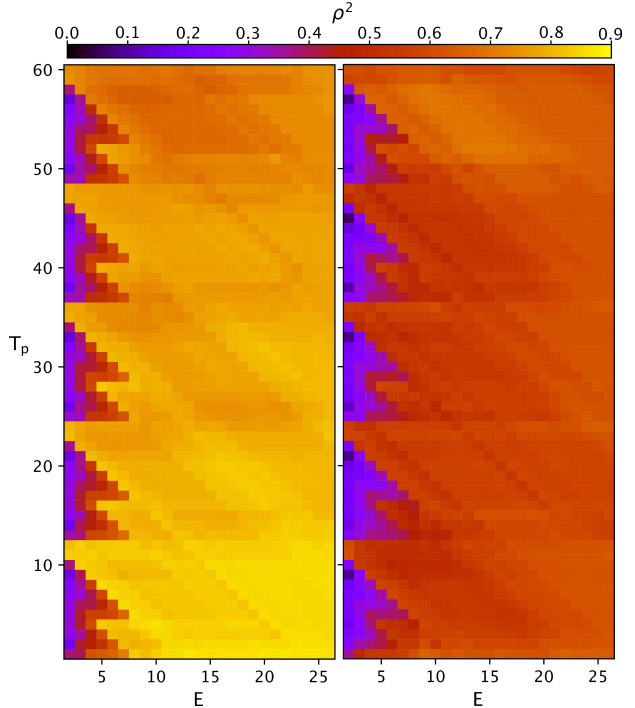


Figure 2: Dynamics as characterized by $\rho^2(E, T_p)$ for *Hieronyma moritziana* species: flowers (left) and fruits (right).

Full plots of $\rho(E, T_p)$ can be very informative about the dynamic state of a system. In figure 2 we show $\rho(E, T_p)$ for *Hieronyma moritziana* species, and some features emerge: only for $E < 12$ the seasonal scale appears, and there are triangular patterns that repeat themselves each 12 months. For flowers and $E > 12$ we obtain a decay in ρ with increasing T_p , while for fruits and $E > 12$ we can observe a recurrence of period around 60 months, which suggest an “*el niño*” coupling [3]. Other species have no structure in parameter space (like figure 5) or some distorted triangular patterns, see figure 3.

For comparison and reference we show in figure 4 (left) $\rho^2(E, T_p)$ plots for chaotic time series with different Lyapunov exponents [5]. It can be appreciated that the intersection points on the E and T_p axes are the same, and that the larger the Lyapunov exponent the smaller those intersection points. Similar triangular patterns were obtained for *Hieronyma moritziana* like species [3] but with a major difference (see figure 2): for several species we have obtained a kind of inversion and repetition of the triangular patterns obtained for chaotic series, which prompts the question: how can we obtain low prediction quality at short times and high prediction quality at longer times?. We have found that a random decay process with resin-

section [4] produces the same kind of triangular patterns obtained for *Hieronyma moritziana* like species, this result is shown in figure 4 (right). We have generated a random decay signal with the explicit functions of González *et al*: $X_n = \sin^2(\theta\pi z^n)$, with parameter $z = p/q$, p and q being relative primes ($q > p$, $z < 1$) [5]. A random decay with reinsertion sounds very *ecosystemic* indeed. We get poor prediction at short times because is a random process, and we obtain a high prediction quality at longer times because once the signal has decayed to near zero values the dynamic is very predictable. It can be observed in figure 2 that for *Hieronyma moritziana* and within one year we obtain a kind of superposition of two triangles, corresponding to two overlapping random decay processes: wet and dry periods of the year in the Venezuelan forest [3]. A simpler plot like the one shown in figure 4 (right) highlights the underlying proposed mechanism. Since we have random decay processes of size 6, it can be said that the case $E = 7$ (see figure 1) is the smaller dimensionality value E outside the *small dimensionality* region in parameter space.

In figure 5 we verify, with the help of the GHWS model [6], that an ideal gas type of dynamics would produce very small values of ρ^2 , for most E and T_p values. The signal

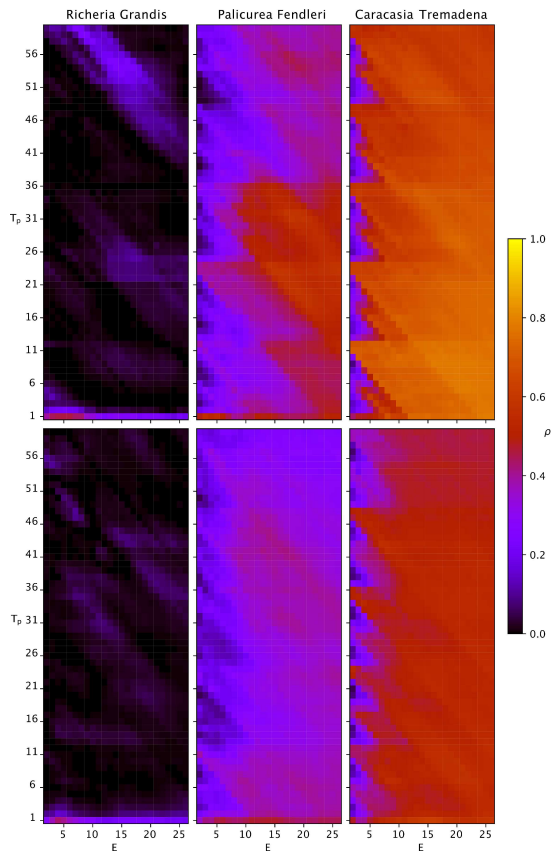


Figure 3: Three cases for population dynamics with very different predictability patterns in parameter space. Up: flowers, Bottom: fruits. See also [3].

used in this case was the *activity* in the system as a function of time [6, 7, 8].

In figures 6 and 7 we show a $\rho^2(E, T_p)$ plot for the atoms coordinates of a protein obtained with molecular dynamics simulations [9, 10, 11]. As an example, we have chosen a typical intrinsically disordered protein such as alpha synuclein associated with neurodegenerative Parkinson's disease, which is known for its complex dynamic conformational behavior and tendency to form aggregates [12]. This protein is made up of three domains or regions known as the N-terminal, NAC, and C-terminal domains [13]. The signal to be processed in this case is the position of the atoms in one of the three regions of the alpha synuclein protein, for a given time. As time passes towards equilibrium the protein jumps between very different dynamic states: fully *disarmed* ($\rho \sim 0$ for most E and T_p), *rigid* (high values of ρ for most E and T_p), a chaotic-like structure (triangular pattern), see figure 6, and several more complicated $\rho(E, T_p)$ patterns. It is important to note that structural disorder has been highlighted recently for alfa

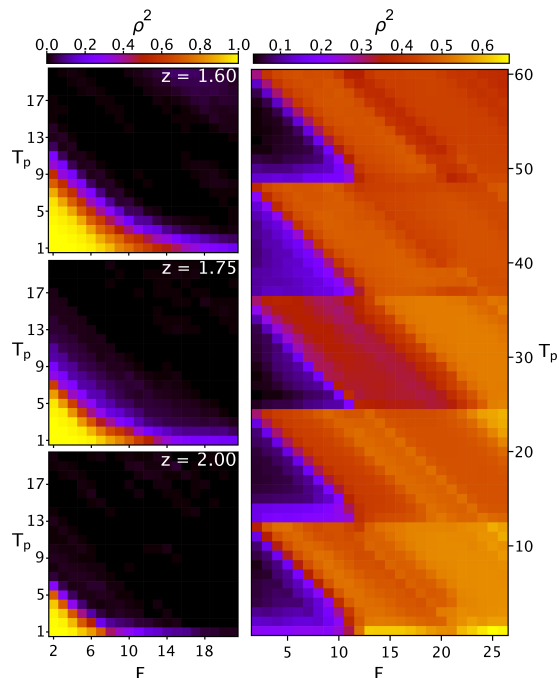


Figure 4: *left*: $\rho^2(E, T_p)$ for chaotic dynamics with different Lyapunov exponents λ . From top to bottom: $z = 1.6, 1.75, 2.0$, with $\lambda = \log z$ [5]. Similar results were obtained for the logarithmic map. *right*: $\rho^2(E, T_p)$ for synthetic data emulating a random decay process with reinsertion. We have used $z = 2/3$ in the explicit functions of references [5] for the random decay process. See text.

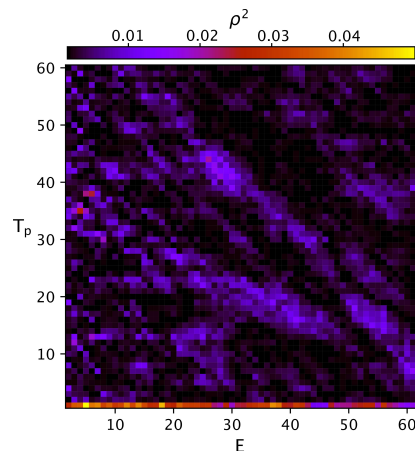


Figure 5: $\rho^2(E, T_p)$ for an ideal gas like dynamics. The processed signal was generated from the GHWS model [6] in a zone of parameter space that produces zero average correlations of activity (see [8], section 3.6), which results in the ideal gas equation of state [7].

synuclein wild type [14], and that we are associating predictability (large values of ρ^2) with rigidity through lost of effective degrees of freedom. A particular pattern emerges for an alpha synuclein dimer scenario: we obtain a particular dimension value E_0 for which no prediction can be made about the position of the atoms along the polymer chain, for any value of T_p , see figure 7 (left). Regarding E_0 , we have interpreted this result as implying that there are structures of length E_0 , involving E_0 number of atoms, that appear in the protein (for a given time).

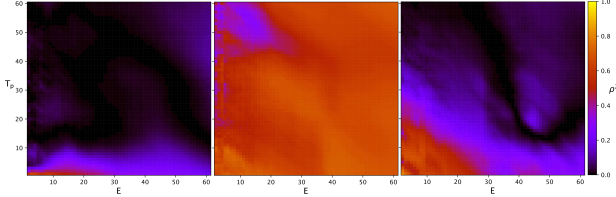


Figure 6: Protein *dynamics*, for data obtained with molecular dynamics simulations [9, 10, 11]. On the left a dynamic state, at a particular time, for which $\rho^2 \sim 0$ for most E and T_p : the protein is *disarmed*. At the center a dynamic state, at a particular time, for which ρ^2 is large for most E and T_p : the protein is *rigid*. To the right we show a chaotic like structure obtained for a particular time (see figure 4 (left) and text).

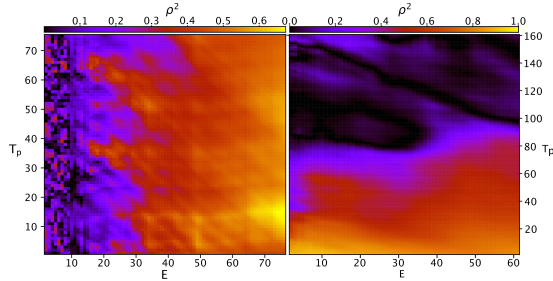


Figure 7: *left*: $\rho^2(E, T_p)$ from protein dynamics, a particular dynamic state for data obtained with molecular dynamics simulations: $\rho^2 \sim 0$ for $E = E_0 \sim 12$, for any T_p considered. *right*: $\rho^2(E, T_p)$ for α -synuclein protein with mutation A53T, after 100ns. The input signal was the y coordinate of the atoms in the N domain.

So far we have shown transient protein dynamics states. In figure 7 (right) we show $\rho^2(E, T_p)$ for the N region of a mutated protein (A53T) after 100ns of simulation. The N-terminal region of the alpha synuclein protein was chosen given its important biological function of binding to the cell membrane [15, 14]. No such state were achieved for the same protein in the wild type case, and this particular dynamic state, a near equilibrium one, fits a chaotic

structure scenario: good predictability for small T_p and eventually unpredictability for large T_p , but with an approximately horizontal frontier between large and near zero values of ρ^2 . These results will be further investigated elsewhere, but let's consider the case of an horizontal frontier (in parameter space) between high and low values of ρ^2 . If we look at figures 1 and 2, we can see that when T_p is a multiple of 12 months ρ^2 shows a weak dependence on dimensionality E , which in turn implies that variations of ρ in parameter space (see below) points only in the T_p direction. This suggest that an approximately horizontal frontier like the one shown in figure 7 (right) could be associated with an interaction with large parts of the protein (the equivalent of *seasonal* scales in this case). Under these considerations we can say that the mutated protein gains some (pathological) rigidity because of self-interaction. Besides, it appears that this pathology could be associated to a lack of cost to make predictions, since the dimensionality parameter E can be directly related to memory capacity which certainly it is expected to have a "cost".

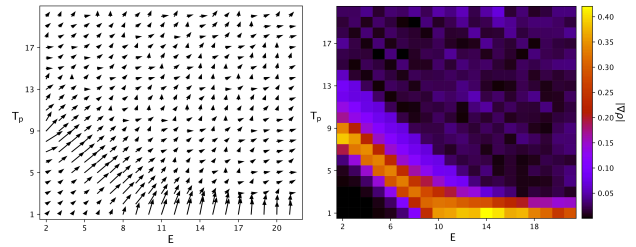


Figure 8: For data obtained from the logistic map we show the vector field $\nabla\rho$ (left) and the modulus of the gradient of ρ in parameter space $|\nabla\rho|$ (right). See text.

Complex adaptive systems. If we were interested in places of parameter space where *adaptation* could be done more efficiently, by changing the dynamic state of the system with minimal variation of parameters, then our ideal spots in parameter space would be places where the gradient (in parameter space) of ρ is large. As an example, in figure 8 we show the modulus and direction of $\nabla\rho$ for the logistic map. We have estimated $\nabla\rho$ from finite differences of parameters values.

From the triangular patterns found for *Hieronyma moritziana* like species in the case of phenology (figure 2) and for chaotic dynamics (figure 4 (left)) it is clear that lines of slope -1 play a role in parameter space (E, T_p). The relation $T_p = E - 1$ is significant in the method introduced by May and Sugihara: it limits the amount of information that in principle could be found in vectors of the form $(x_i, x_{i-1}, x_{i-2}, \dots, x_{i-(E-1)})$ when trying to make a prediction about x_{i+T_p} . The lines of slope -1 are perpen-

dicular to lines of the form $T_p = E - 1$, which suggests that the direction in parameter space given by $\nabla\rho$, as can be seen in figure 8, is very relevant in this method, which also highlights the natural framework it provides for considering *adaptation* in Complex Systems, as commented in the previous paragraph.

We have presented results for several types of system-dynamics based on the forecasting method introduced by May and Sugihara [1]. Our results highlight the powerfulness of full plots of $\rho(E, T_p)$ obtained with the nonlinear forecasting method to analyze and characterize the dynamics of Complex Systems, for *scales* as large as forest Ecosystems and as small as Proteins.

References

- [1] G. Sugihara and R. M. May, *Nonlinear forecasting as a way of distinguishing chaos from measurement error in time series*, Nature volume 344, pages 734–741 (1990).
- [2] Andreja Bubic, D. Yves von Cramon and Ricarda I. Schubotz, *Prediction, cognition and the brain*, Frontiers in Human Neuroscience, Volume 4 , Article 25, March 2010.
- [3] Saúl Flores, Matthew L. Forister, Hendrik Sulbaran, Rodrigo Díaz and Lee A. Dyer, *Extreme drought disrupts plant phenology: Insights from 35 years of cloud forest data in Venezuela*, Ecology, Volume 104, Issue 5, May 2023, e4012.
- [4] H. G. Schuster, *Deterministic Chaos: An Introduction* (Fourth edition), Wiley-VCH, 2005. See Chapter 5, fig. 58.
- [5] J. A. González y L. B. Carvalho, *Analytical Solutions to Multivalued Maps*, Mod. Phys. Lett. B 11, 521 (1997); J. A. González, L. I. Reyes y L. E. Guerrero, *Exact solutions to chaotic and stochastic systems*, Chaos 11, 1 (2001).
- [6] Leonardo Reyes and David Laroze, *Cellular Automata for excitable media on a Complex Network: The effect of network disorder in the collective dynamics*, Physica A 588 (2022) 126552.
- [7] Parameter values for the GHWS model in figure 5: $K = 6$, $\sigma = 2.4$, $z = 5$, $N = 1000$. After $T = 1000$ steps we got the fluctuations in activity from the next 1000 steps. For these parameter values the normalized fluctuations $\zeta = N(\langle F^2 \rangle - \langle F \rangle^2) / [\langle F \rangle(1 - \langle F \rangle)]$ are ≈ 1 , where F is the activity [6]. $\zeta \approx 1$ is equivalent to say that the dynamics is an ideal gas like one (see [8], section 3.6).
- [8] David Chandler, *Introduction To Modern Statistical Mechanics*, Oxford University Press, 1987.
- [9] Lenin González-Paz, María Laura Hurtado-León, Carla Lossada, Francelys V. Fernández-Materán, Joan Vera-Villalobos, Marcos Loroño, J.L. Paz, Laura Jefeys and Ysaías J. Alvarado, *Structural deformability induced in proteins of potential interest associated with COVID-19 by binding of homologues present in ivermectin: Comparative study based in elastic networks models*, Journal of Molecular Liquids, 340 (2021) 117284.
- [10] Turkan Haliloglu, Ivet Bahar and Burak Erman, *Gaussian Dynamics of Folded Proteins*, Physical Review Letters, Vol. 79, Number 16, 3090 (1997); Ivet Bahar, Ali Rana Atilgan and Burak Erman, *Direct evaluation of thermal fluctuations in proteins using a single-parameter harmonic potential*, Folding & Design, 07 May 1997, 2:173–181.
- [11] GROMACS: [https://www.softxjournal.com/article/S2352-7110\(15\)00005-9/fulltext](https://www.softxjournal.com/article/S2352-7110(15)00005-9/fulltext)
WebGRO for Macromolecular Simulations: <https://simlab.uams.edu/>
- [12] Surabhi Mehra, Shruti Sahay, Samir K Maji, *α -Synuclein misfolding and aggregation: Implications in Parkinson’s disease pathogenesis*, Biochim. Biophys. Acta Proteins. Proteom. 1867(10):890-908 (2019).
- [13] Natalia P. Alza, Pablo A. Iglesias González, Melisa A. Conde, Romina M. Uranga, Gabriela A. Salvador, *Lipids at the Crossroad of α -Synuclein Function and Dysfunction: Biological and Pathological Implications*, Frontiers in Cellular Neuroscience, 13: 175 (2019) .
- [14] Soumik Ray, Nitu Singh, Rakesh Kumar, Komal Patel, Satyaprakash Pandey, Debalina Datta, Jaladhar Mahato, Rajlaxmi Panigrahi, Ambuja Navalkar, Surabhi Mehra, Laxmikant Gadhe, Debdeep Chatterjee, Ajay Singh Sawner, Siddhartha Maiti, Sandhya Bhatia, Juan Atilio Gerez, Arindam Chowdhury, Ashutosh Kumar, Ranjith P adinhateeri, Roland Riek, G. Krishnamoorthy, Samir K. Maji, *α -Synuclein aggregation nucleates through liquid–liquid phase separation*, Nature Chemistry, 12, 705 – 716 (2020).
- [15] Giuliana Fusco, Alfonso De Simone, Tata Gopinath Vitaly Vostrikov, Michele Vendruscolo, Christopher M. Dobson, Gianluigi Veglia, *Direct observation of the three regions in α -synuclein that determine its membrane-bound behaviour*, Nature Communications, 5, 3827 (2014).